AIAA JOURNAL
Vol. 34, No. 11, November 1996

Efficient Foil Propulsion Through Vortex Control

Knut Streitlien* and George S. Triantafyllou†
City College of the City University of New York, New York, New York 10031
and
Michael S. Triantafyllou‡
Massachusetts Institute of Technology, Cambridge, Massachusetts 02139

We investigate the problem of a heaving and pitching hydrofoil in an inflow that consists of a uniform velocity field and a staggered array of vortices. The foil can exploit the energy in such a Kármán vortex street for efficient propulsion of animals or submarines. Through a two-dimensional inviscid analysis, we find that the phase between foil motion and the arrival of inflow vortices is a critical parameter. Everything else being equal, the highest efficiency is seen when this phase is such that the foil moves in close proximity to the oncoming vortices. Different modes of vortex interaction in the wake results from a variation in this phase, and we show that the flow downstream of the foil is related to the foil input power.

Nomenclature

A_n	= Glauert series coefficients, $n = 0, 1, 2, 3, \ldots$
b	= x location of pitch axis
C	= Theodorsen function
c	= foil half-chord
D	= drag associated with inflow vortex street
d	= width of inflow vortex street
h	= instantaneous heave displacement, positive up
h_0	= heave amplitude
i	= imaginary unit
J_n	= Bessel function of the first kind, order n
L	= lift, positive upwards; instantaneous in simulation, complex amplitude in linear theory
l	= spatial period of inflow vortex street
M	= moment, positive counterclockwise; instantaneous about pitch axis in simulation, complex amplitude about midchord in linear theory
P	= instantaneous input power
T	= instantaneous thrust
t	= time
U	= freestream velocity
U_c	= convection velocity of Kármán vortex street
U_0, V_0	= approximate velocity at centerline of Kármán vortex street
(x, y)	= coordinate system in mean foil position
α	= instantaneous pitch angle, positive counterclockwise
α_0	= pitch amplitude
Γ	= circulation of incident vortices
η	= efficiency
ξ	= energy recovery factor
σ	= reduced frequency $\omega c/U$
σ_c	= reduced frequency $\omega c/U_c$
σ_0	= reduced frequency $\omega c/U_0$
ϕ	= phase between inflow and foil motion
ψ	= phase between heave and pitch
ω	= frequency
$\langle\,\rangle$	= average over one period in time
$\cdot$	= time derivative

Received May 1, 1995; revision received June 17, 1996; accepted for publication July 16, 1996; also published in *AIAA Journal on Disc*, Volume 2, Number 1.

*Research Associate, Levich Institute, Steinman Hall 1M11, Convent Avenue and 140th Street. Member AIAA.
†Professor, Levich Institute and Department of Mechanical Engineering, Steinman Hall 1M16, Convent Avenue and 140th Street.
‡Professor, Department of Ocean Engineering, Room 5-323, 77 Massachusetts Avenue.

Introduction

CONVENTIONAL propulsion devices used for marine vessels are adversely affected by unsteady or nonuniform inflow conditions. Aquatic animals, on the other hand, need not be negatively affected by such disturbances, as they propel themselves by undulatory motions of lifting surfaces. Here, the possibility exists that energy in the inflow can be used constructively, with a resulting improvement in mechanical efficiency. Recently, Triantafyllou and Triantafyllou[1] gave evidence that swimming fish can manipulate ambient vorticity with their caudal (tail) fin and that this is a mechanism through which they can extract energy that would otherwise be left in the wake. Such vortex control may help explain the remarkable swimming capacity observed among marine animals and lead to efficient propulsion systems for submarine robots, which must cover large distances on their own battery power. The discussion in this paper pertains to those species that have developed high aspect ratio caudal fins, which includes the most prominent swimmers,[2] thus permitting a two-dimensional analysis of the isolated fin in a freestream. No assumption is made as to the source of the inflow disturbances; they could be caused by foreign objects, other specimens (as in a school of fish), or even the upstream parts of the fish itself. The problem at hand is therefore to study the propulsive effectiveness and flow characteristics for a foil heaving and pitching:

$$h = h_0 \cos(\omega t - \phi) \tag{1}$$

$$\alpha = \alpha_0 \cos(\omega t - \phi - \psi) \tag{2}$$

in a stream that varies in space and time. In nature and technology, the Kármán vortex street is a ubiquitous periodic flow, and it is quite natural to choose a vortex street as the model inflow. The numerical and theoretical analyses presented here complement the experimental studies of Gopalkrishnan et al.,[3] where a foil was made to perform a prescribed heave and pitch motion while placed in a vortex street generated by a cylinder. These experiments showed that the propulsive efficiency and vorticity patterns in the wake were sensitive to the phase between the oncoming vortices and the foil motion. This sensitivity is the focus of our work. By wake we mean any flow disturbance downstream from a solid object, whether the velocity profile is of the usual wake type or not. We will also distinguish between the term vortex street, which can be any array of concentrated vorticity, and Kármán vortex street, the theoretical idealization into an infinite staggered array of alternate sign point vortices.

We define the problem in the context of ideal flow. The Kármán vortex street translates with velocity:

$$U_c = U - (\Gamma/2l)\tanh(\pi d/l) \tag{3}$$

For the problem to be a steady harmonically oscillating one, ω must coincide with the vortex encounter frequency:

$$\omega = 2\pi U_c / l \tag{4}$$

Time t is always adjusted such that a vortex passes the y axis in the upper half-plane at $t = 0$; consequently the phase between the foil motion and oncoming vortex street is determined by ϕ. There are eight nondimensional groups spanning the input parameter space in this problem:

$$\omega c/U,\ d/c,\ \Gamma/(U_c),\ h_0/c,\ b/c,\ \psi,\ \alpha_0,\ \phi \tag{5}$$

From numerical or analytical analysis, we obtain the reaction forces experienced by the foil as functions of time, $T(t)$, $L(t)$, and $M(t)$. The instantaneous input power to the foil is

$$P = -L\dot{h} - M\dot{\alpha} \tag{6}$$

For most applications, the primary performance parameter is hydromechanical efficiency, conventionally defined as the ratio of average useful work to average input work:

$$\eta = \langle T \rangle U / \langle P \rangle \tag{7}$$

We note that efficiency defined this way can be made arbitrarily high by letting the motion amplitudes become small, because the nonuniform inflow will result in a finite mean thrust through leading-edge suction, while the input power is arbitrarily small. In cases where η exceeds unity, it may be more relevant to consider the fraction of inflow energy that the foil recovers:

$$\xi = \frac{U\langle T \rangle - \langle P \rangle}{U\langle D \rangle} \tag{8}$$

where $\langle D \rangle$ is the mean drag force associated with the vortex street[4] (unit fluid density assumed):

$$\langle D \rangle = (\Gamma d/l)(2U_c - U) + (\Gamma^2/2\pi l) \tag{9}$$

Equation (8) is therefore the ratio of net power gain by the foil to the power required to sustain the incoming vortex street.

Our numerical algorithm has been presented elsewhere[5–7] and shares many basic features with those of other authors,[8–10] and so only a brief discussion is given here. By conformal transformation of a circle to a Joukowski profile we find the velocity potentials that correspond to surge, heave, and pitch of the foil in a local coordinate system. The circle theorem allows for additional potentials that represent point vortices, which completes the description of the flow due to a moving Joukowski profile in the presence of point vortices. In particular, we can find the convection velocity of the vortices themselves, according to Routh's rule.[11] New vortices are released both at the trailing edge at every time step and upstream at every half-period, in such a way that the Kutta condition and Kelvin's theorem are satisfied. This models the foil trailing vortex sheet and the oncoming vortex street, which are allowed to evolve nonlinearly in time. In Ref. 7 we demonstrated how the force and moment expressions given by Milne Thomson[12] can be integrated over the foil surface, resulting in expressions for L, M, and T that consist of added mass forces and vortex forces.

The upstream vortices are released in circular patches of alternate sign at $y = \pm d/2$, at some fixed $x < 0$. Each patch has a number of point vortices distributed evenly over the area. The streamwise distance between the released vortices, l, is a function of U, Γ, ω, and d. Equation (4) has two solutions for l, and it appears that the simulated vortex street always takes on the highest of these. There is an artifact in the force record from the sudden introduction of upstream vortices, but the effect diminishes as we move the release points farther upstream. We found that 15 chord lengths was sufficiently far upstream to make this artifact negligible.

We have also formulated an analytical method, valid when certain nondimensional groups of input parameters are asymptotically small. It combines different elements of the linear unsteady airfoil theory of von Kármán and Sears[13] and Sears.[14] A similar extension was given by Wu,[15] who solved for the optimum motion of a foil placed in a shallow water free surface wave. Linear theory is valid in the limit of zero foil camber and thickness, displacements, and flow perturbations, and requires only that we supply the undisturbed vertical flow velocity at the foil location, as observed in a reference frame fixed to the foil.

We start by assuming that the oncoming flow is the classical Kármán vortex street. If undisturbed, it would produce the following complex flow velocity along the centerline:

$$[u - iv]_{y=0} = U + \frac{i\Gamma}{l}\frac{\cosh(\pi d/l)}{\sin\{[2\pi(x - U_c t)]/l\} - i\sinh(\pi d/l)} \tag{10}$$

For small l/d, this velocity field takes the form of a vertical sinusoidal gust on a uniform horizontal stream:

$$U_0 = U - \frac{\Gamma}{l} \tag{11}$$

$$V_0 = -\frac{2i\Gamma}{l} e^{-(\pi d/l)} e^{-(i\omega x/U_c)} e^{i\omega t} \tag{12}$$

In Eq. (12) and in the sequel, i refers to harmonic time dependence, and whenever an expression has the factor $e^{i\omega t}$, it is implied that the real part of the whole expression should be taken. The total upwash at the foil is due to V_0 and the heave and pitch motion. When this upwash is expressed as a Fourier series in the inverse cosine of the foil coordinate, the so-called Glauert series, it turns out that the first four coefficients, $A_0, \ldots, A_3$, are sufficient to determine the foil response. In the present notation, they become

$$A_0 = -\frac{2i\Gamma}{U_0 l} e^{-(\pi d/l)} J_0(\sigma_c) + \left[i\omega \frac{-h_0 + \alpha_0 b e^{-i\psi}}{U_0} - \alpha_0 e^{-i\psi} \right] e^{-i\phi} \tag{13}$$

$$A_1 = -\frac{2\Gamma}{U_0 l} e^{-(\pi d/l)} J_1(\sigma_c) - \frac{i\alpha_0\sigma_0}{2} e^{-i(\psi+\phi)} \tag{14}$$

$$A_2 = \frac{2i\Gamma}{U_0 l} e^{-(\pi d/l)} J_2(\sigma_c) \tag{15}$$

$$A_3 = \frac{2\Gamma}{U_0 l} e^{-(\pi d/l)} J_3(\sigma_c) \tag{16}$$

Von Kármán and Sears obtained the complex amplitudes for lift (positive upwards) and moment about $x = 0$ (positive counterclockwise) expressed in the Glauert coefficients:

$$L = i\pi\sigma_0 U_0^2 c(A_0 - A_2) + 2\pi U_0^2 c(A_0 + A_1)C(\sigma_0) \tag{17}$$

$$M = i\pi\sigma_0 U_0^2 c^2 (A_1 - A_3)/4 + \pi U_0^2 c^2 \{-A_0 C(\sigma_0) + A_1[1 - C(\sigma_0)] + A_2\} \tag{18}$$

Now the average input power, according to Eq. (6), is simply

$$\langle P \rangle = \mathrm{Re}\{i\omega e^{i\phi}(e^{i\psi}\alpha_0 b - h_0)L - i\omega\alpha_0 e^{i(\psi+\phi)}M\}/2 \tag{19}$$

Furthermore, the leading-edge suction can be found by a local momentum consideration (Ref. 4, p. 52), and the average thrust follows (with a contribution from the lift inclined with the angle of attack):

$$\langle T \rangle = \pi c U_0^2 |A_0 C(\sigma_0) - A_1[1 - C(\sigma_0)]|^2 + \mathrm{Re}\{L\alpha_0 e^{i(\psi+\phi)}\}/2 \tag{20}$$

The efficiency η and energy recovery factor ξ follow from Eqs. (7) and (8).

We have found that the restriction $l/d \to 0$ can be relaxed quite a bit in this theory; l/d does not need to be very small for the theory to agree with simulation. But the restriction of small foil motion amplitude is much stricter than in the case of uniform inflow, for two reasons. First, as soon as the foil displacement becomes more than a small fraction of $d/2$, the foil moves in regions where the inflow is no longer independent of y, as assumed earlier. Second, when the foil gets close to the inflow vortices, the assumption that the vortex street is undisturbed is no longer justified.

Results

The numerical results are presented as graphs of $\langle T \rangle$, $\langle P \rangle$, and η, vs ϕ, for different combinations of the input parameters, which are listed in Table 1. The significance of ϕ is shown as part of Fig. 1, where we note that $\phi = 0$ results in close interaction between foil and vortices, whereas for $\phi = \pm\pi$ the interaction is minimal.

For reference, case 1 was chosen to be similar to the experiment in Ref. 3 as far as possible. Figure 1 shows that the experimentally observed efficiency is somewhat lower than the numerical results. This could be due to viscosity (leading-edge separation), three-dimensional flow, or uncertainty in the inflow parameters. In regard to the latter, we should mention that the parameters of the oncoming vortex street were not obtained during the force measuring experiment. Instead they were found by our colleague J. Anderson using the digital particle image velocimetry technique in a smaller, but geometrically similar, setup. Given that the efficiency is sensitive to the strength and width of the oncoming vortex street, the agreement between experiment and simulation must be considered satisfactory. In particular we note that the trends in $\eta(\phi)$ agree, with maxima and minima at the same values of ϕ. In the experiment, ϕ was controlled by placing the foil at different distances behind the vortex generating cylinder, hence the lack of periodicity.

Figure 2 shows the results for the other seven cases, where we systematically varied the input parameters. The most striking feature is the consistent dependence on ϕ, in all but case 6. Apart from this case, the close interaction mode, $\phi = 0$, always leads to the highest values of thrust and input power. The ratio between them is such that efficiency reaches a maximum at this point as well. This characteristic was also seen in the experiment. The pressure distribution that results from the foil interacting closely with the oncoming vortex street appears to be favorable in the context of propulsion, with respect to both producing the required thrust and doing so effectively. Case 6 has a very strong vortex street that undergoes large self-induced deformation when interacting with the foil, which is probably why it behaves differently from the others.

Table 1 Input for simulations[a]

Case	h_0	α_0	b	ω	Γ	d
1	0.833	0.785	−0.333	1.24	2.23	3.0
2	0.4	0.2	0	$\pi/3$	$\pi/5$	2.0
3	0.4	0.2	0	$\pi/3$	$2\pi/5$	2.0
4	0.9	0.3	0	$\pi/3$	$2\pi/5$	3.6
5	0.9	0.3	0	$\pi/3$	$2\pi/5$	1.8
6	0.4	0.2	0	$\pi/3$	$4\pi/5$	3.0
7	0.4	0.2	−1	$\pi/3$	$2\pi/5$	2.0
8	0.4	0.2	1	$\pi/3$	$2\pi/5$	2.0

[a]In all cases we set $U = 1$, $\rho = 1$, $c = 1.008$, thickness $= 12\%$, $\psi = \pi/2$, and radius of the upstream patches $= 0.5$.

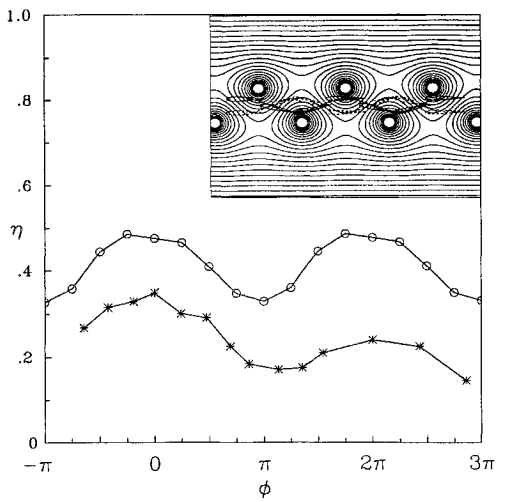

Fig. 1 Efficiency vs phase angle ϕ for ○, simulation and ∗, experiment. The inset shows the streamlines of the vortex street and typical paths of the foil, as seen by an observer moving with the vortices: ——, $\phi = 0$ and – – –, $\phi = \pm\pi$.

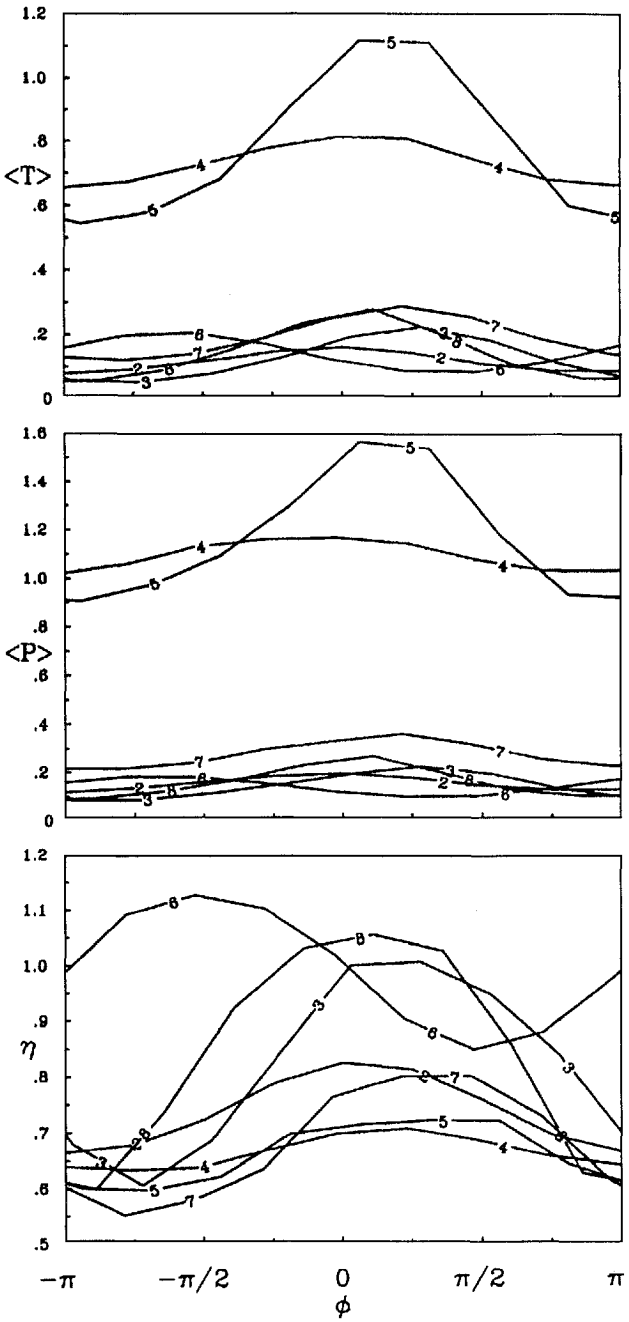

Fig. 2 Mean values for input power, thrust, and efficiency vs phase angle ϕ for cases 2–8. Because U, c, and ρ are all unity, $\langle T \rangle$ and $\langle P \rangle$ are effectively nondimensionalized.

Aside from such nonlinear effects, the effect of increasing Γ is to make the vortex induced forces on the foil larger, thrust more than input power, such that efficiency increases. It also makes the dependency on ϕ stronger, which is quite natural considering the fact that efficiency cannot depend on ϕ in the limit of zero vortex strength. For low foil motion amplitudes and moderately high Γ, η can exceed unity, but we were never able to achieve more than modest energy recovery factor, $\xi = 2\%$. The two last cases show the dependence on pitch axis location. The results indicate that shifting this point toward the trailing edge is advantageous, just as in the case for a foil in uniform inflow.[2]

The dependence on foil motion amplitude is more complicated than for the other parameters. If h_0 increases, while still remaining small compared with the width of the vortex street, the dependence on ϕ becomes weaker, and maximum efficiency goes down. This is because the vortex induced pressure variation loses significance compared with that caused by the foil motion, and the situation is more like that of a foil in uniform flow. But when h_0 is high,

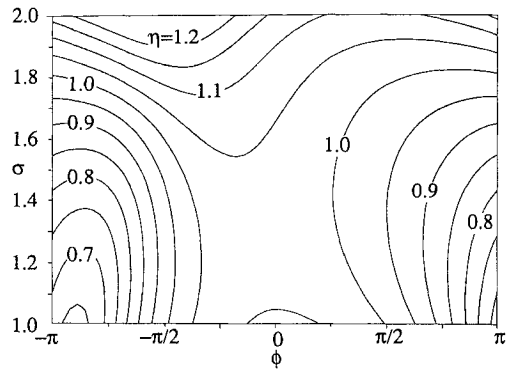

Fig. 3 Contour plot of efficiency vs phase angle ϕ and reduced frequency σ according to the linear theory. Otherwise like case 3.

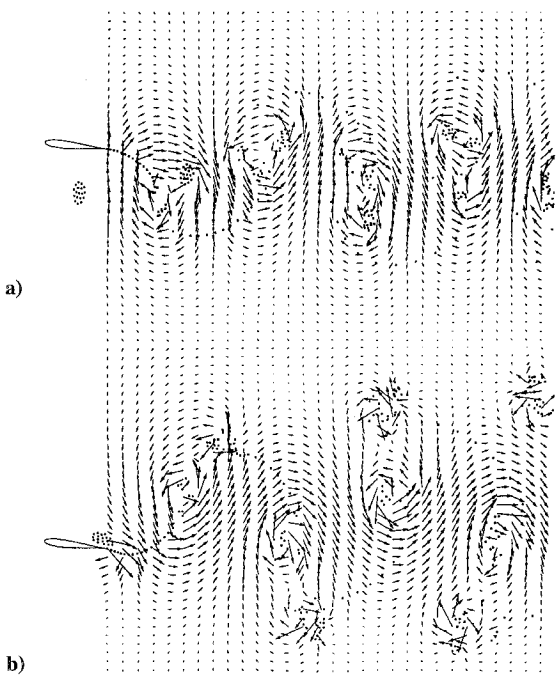

Fig. 4 Vector plot of flow velocity for case 5 for the values of ϕ that give a) minimum and b) maximum input power. The velocity field of each computational vortex element has been mollified to avoid infinite local velocities.

nonlinear interactions give rise to different dependencies. In case 5, for example, heave double amplitude is nominally equal to the vortex street width, and variations in ϕ lead to entirely different interaction modes. At $\phi = \pm\pi$, the foil moves among the vortices as usual, but as ϕ gets smaller, the finite size of the vortices and their tendency to convect toward the foil under the influence of their images inside the foil cause the foil to plunge right through the vortices for certain ϕ. For ϕ near 0, the vortices are actually sucked to the opposite side the foil because of their oppositely signed images in the foil. The resulting thrust and power can be very high.

In the interest of brevity, we did not present linear theory results for the problems discussed earlier. Briefly, the theory agrees with simulation to within 0.1 for η in cases 2, 3, 7, and 8, where the foil motion amplitudes and vortex strengths are moderate. For the other cases, the agreement is less satisfactory. So at least in the region of the parameter space where we expect it to be valid, the theory confirms the conclusions drawn earlier. However, the usefulness of the theory goes beyond mere confirmation of the numerical results. Figure 3 shows analytically predicted efficiency vs reduced frequency over a range that would require extensive simulation to cover. It is evident that the typical dependence on ϕ, with a maximum around $\phi = 0$, is consistent throughout the range of frequencies.

The qualitative features of the wake for different vortex–foil interaction modes is also of interest. Basic conservation laws tell us that the kinetic energy in the wake flow is related to the mean input power $\langle P \rangle$. During one period, $2\pi/\omega$, the kinetic energy that crosses a vertical line downstream of the foil must amount to the kinetic energy that crosses a line upstream of the foil, plus the work that is done by the foil on the fluid, $\langle P \rangle 2\pi/\omega$. [The kinetic energy of the instantaneous velocity field associated with point vortices is not defined, but the energy input over one period has meaning, e.g., the denominator of Eq. (8) in the case of a Kármán vortex street.] Thus, changes in the phase ϕ, which lead to different values of $\langle P \rangle$, ought to result in wakes that are qualitatively different. We have tested this hypothesis for case 5, which has the largest variation in $\langle P \rangle$ as a function of ϕ. The instantaneous wake velocity fields (in a frame of reference fixed in the fluid at rest) for $\phi = \pi$ and 0 are shown in Fig. 4. The two vector fields are quite different, the high-power wake being much wider, with a strong streamwise velocity component. It forms a continuous meandering stream in the center of the wake, compared with the smaller downstream velocity component and narrower width of the low-power wake. These differences are also consistent with the large differences in average thrust between the two values of ϕ, because thrust is in part associated with momentum flux. Wakes with a reduced signature such as in Fig. 4a are interesting in the context of stealthworthiness of submarines. One might imagine that an underwater robot could swim in the high thrust mode normally (Fig. 4b) and switch to a stealth mode (Fig. 4a) when desirable.

Conclusions

From observations of fast swimming species in the animal kingdom we know that the flapping hydrofoil can be a very effective means of propulsion. There is also evidence suggesting that fish can manipulate the vorticity by skillful use of the caudal fin. In this report we have tried to answer the following questions: how does the foil interact with such ambient concentrations of vorticity, and what potential benefits can be reaped from such interactions? Our quantitative results are in the form of a parameter study of the conventionally defined propulsive efficiency. We found that efficiency can exceed 100% when the foil motions are on the order of half the vortex street width and the vortex street is strong enough to correspond to a drag coefficient of 0.4. In all but one case we found that the timing, or phase, of the foil motion should be such that it is brought in close contact with the individual vortices in the inflow, a fact that is also indicated by previously published experiments. We also considered whether the foil could regain a net amount of energy from the oncoming flow. This is indeed the case during optimal conditions, although the net gain is small compared with the energy in the Kármán vortex street.

The structure of the flow in the combined wake downstream of the foil is also of interest. A variety of interaction modes can be obtained by adjusting the parameters that control foil motion. Different energy levels in the combined wake are associated with different input power to the foil.

Acknowledgment

The authors gratefully acknowledge financial support by the Office of Naval Research.

References

[1]Triantafyllou, M. S., and Triantafyllou, G. S., "An Efficient Swimming Machine," *Scientific American*, Vol. 272, No. 3, 1995, pp. 64–70.

[2]Lighthill, J., *Mathematical Biofluiddynamics*, Society for Industrial and Applied Mathematics, Philadelphia, PA, 1975.

[3]Gopalkrishnan, R., Triantafyllou, M. S., Triantafyllou, G. S., and Barrett, D., "Active Vorticity Control in a Shear Flow Using a Flapping Foil," *Journal of Fluid Mechanics*, Vol. 274, Sept. 1994, pp. 1–22.

[4]Von Kármán, T., and Burgess, J. M., "General Aerodynamic Theory—Perfect Fluids," *Aerodynamic Theory*, edited by W. F. Durand, Vol. 2. Springer–Verlag, Berlin, 1935, pp. 52, 346–349.

[5]Streitlien, K., "A Simulation Procedure for Vortex Flow over an Oscillating Wing," Massachusetts Inst. of Technology, M.I.T. Sea Grant, MITSG 94-7, Cambridge, MA, Jan. 1994.

[6]Streitlien, K., "Extracting Energy from Unsteady Flows Through Vortex Control," Ph.D. Thesis, Dept. of Ocean Engineering, Massachusetts Inst. of Technology/Woods Hole Oceanographic Institution, Cambridge, MA, 1994.

[7]Streitlien, K., and Triantafyllou, M. S., "Force and Moment on a Joukowski Profile in the Precense of Point Vortices," *AIAA Journal*, Vol. 33, No. 4, 1995, pp. 603–610.

[8]Sarpkaya, T., "An Inviscid Model of Two-Dimensional Vortex Shedding for Transient and Asymptotically Steady Separated Flow over an Inclined Plate," *Journal of Fluid Mechanics*, Vol. 68, No. 1, 1975, pp. 109–128.

[9]Choi, D. H., and Landweber, L., "Inviscid Analysis of Two-Dimensional Airfoils in Unsteady Motion Using Conformal Mapping," *AIAA Journal*, Vol. 28, No. 12, 1990, pp. 2025–2033.

[10]McCune, J. E., and Tavares, T. S., "Perspective: Unsteady Wing Theory—The Kármán/Sears Legacy," *Journal of Fluids Engineering*, Vol. 115, No. 4, 1993, pp. 548–560.

[11]Sarpkaya, T., "Computational Methods with Vortices—The 1988 Freeman Scholar Lecture," *Journal of Fluids Engineering*, Vol. 111, No. 1, 1989, pp. 5–52.

[12]Milne Thomson, L. M., *Theoretical Hydrodynamics*, 4th ed., Macmillan, New York, 1960, pp. 244–247.

[13]Von Kármán, T., and Sears, W. R., "Airfoil Theory for Non-Uniform Motion," *Journal of the Aeronautical Sciences*, Vol. 5, No. 10, 1938, pp. 379–390.

[14]Sears, W. R., "Some Aspects of Non-Stationary Airfoil Theory and Its Practical Application," *Journal of the Aeronautical Sciences*, Vol. 8, No. 3, 1941, pp. 104–108.

[15]Wu, T. Y., "Extraction of Flow Energy by a Wing Oscillating in Waves," *Journal of Ship Research*, Vol. 16, No. 1, 1972, pp. 66–77.